Nano Energy 40 (2017) 88–94

Contents lists available at ScienceDirect

Nano Energy

journal homepage: www.elsevier.com/locate/nanoen

Communication

# Nitrogen-doped hollow porous carbon polyhedrons embedded with highly dispersed Pt nanoparticles as a highly efficient and stable hydrogen evolution electrocatalyst

Jie Ying[a], Gaopeng Jiang[a], Zachary Paul Cano[a], Lei Han[a], Xiao-Yu Yang[b], Zhongwei Chen[a,*]

[a] Department of Chemical Engineering, University of Waterloo, Ontario, Canada N2L 3G1
[b] State Key Laboratory Advanced Technology for Materials Synthesis and Processing, Wuhan University of Technology, 122, Luoshi Road, Wuhan 430070, China

ARTICLE INFO

*Keywords:*
Platinum nanoparticles
High dispersion
Nitrogen-doping
Hollow porous nanostructures
Hydrogen evolution reaction

ABSTRACT

The hydrogen evolution reaction (HER) is a promising alternative method of producing clean and renewable hydrogen resources. Although Pt-based nanomaterials are the most efficient catalysts for HER, their poor stability and durability strongly impede their practical application. In this study, we report a new, efficient strategy to fabricate highly dispersed Pt nanoparticles within unique nitrogen-doped hollow porous carbon polyhedrons (Pt@NHPCP) derived from polymer coated metal-organic frameworks. Pt@NHPCP displays enhanced HER activity compared to commercial Pt/C. Most importantly, Pt@NHPCP exhibits excellent stability and durability, showing no nanostructure change and negligible activity decrease after 5000 potential cycles. The outstanding HER performance of Pt@NHPCP can be attributed to its unique structural features including highly dispersed Pt, nitrogen-doping, large surface area, hollow nanostructure and hierarchical pore system.

## 1. Introduction

Hydrogen, as an alternative and renewable energy source to reduce dependence on diminishing fossil fuel sources, has attracted significant attention due to its high gravimetric energy density and pollution-free oxidation reaction [1–4]. Currently, hydrogen for industrial applications is mainly generated by reforming of natural gas or methane, which is not sustainable and has the issue of pollutant emission of $CO_2$ [2]. In contrast, electrochemical water splitting is identified as a promising method to cleanly produce hydrogen resources [5–8]. In this regard, tremendous research has been devoted to searching for highly-efficient electrocatalysts for the hydrogen evolution reaction (HER) [9–13]. Although great progress has been achieved for noble-metal-free HER catalysts, platinum (Pt)-based nanomaterials are still the most efficient and commonly used catalysts for HER [8,14,15]. However, Pt's scarcity and high cost, in addition to its vulnerability to aggregation and subsequently drastic reduction in catalytic performance, largely impedes the commercial application of Pt as a catalyst for HER [9,10]. Therefore, sophisticated strategies for synthesizing advanced Pt-based electrocatalysts with enhanced utilization efficiency and prolonged stability and durability are highly demanded.

Carbon materials have been heavily explored as a support to stabilize Pt-based catalysts, owing to their excellent electrochemical properties, stability and low cost. They can also improve the activity of Pt due to the synergistic effect between the catalyst and support [16–18]. Among all carbon materials, hollow porous carbons, possessing the advantages of low density, large surface area, and fast mass transport, are emerging as excellent support materials for the purpose of improving catalyst activity and stability in a variety of catalytic applications [19–23]. Their hollow porous structures can embed, disperse, and protect catalytically-active nanoparticles from leach-out and/or aggregation. In addition, heteroatom dopants such as nitrogen and sulfur introduced into carbon supports can further improve catalyst stability and activity through the improvement of interaction and synergistic effect between the catalyst and support [24–27]. These two concepts have been united through the fabrication of various hollow porous carbons doped with heteroatoms [28–32].

Traditional synthetic approaches to hollow porous carbons encapsulating catalytically-active nanoparticles require hard templates, whose structures can be adjusted to precisely control the final hollow porous structures. However, complicated and harsh conditions are required for hard template removal, such as strongly corrosive acids (e.g. HF) or bases (e.g. NaOH) [19–21]. Soft templates, such as surfactants and organic polymers, have recently emerged as an effective approach to incorporate nanoparticles into hollow porous carbons. These templates can be easily removed using a high-temperature carbonization

* Corresponding author.
*E-mail address:* zhwchen@uwaterloo.ca (Z. Chen).

http://dx.doi.org/10.1016/j.nanoen.2017.07.032
Received 12 June 2017; Received in revised form 15 July 2017; Accepted 19 July 2017
Available online 20 July 2017

process; however, this often yields unevenly dispersed active nanoparticles in the hollow structures [23]. Therefore, a new, efficient approach to synthesize and disperse metal nanoparticles inside hollow porous carbons is required in the pursuit of a high-performance and commercially-viable HER catalyst. The desired strategy must (i) allow for safe and straightforward template removal, (ii) provide an abundant source of heteroatom dopants and (iii) create a highly dispersed matrix of embedded nanoparticles with the purpose of maximizing catalytic activity, stability, durability, and utilization efficiency.

Herein we present a facile and efficient method to prepare Pt nanoparticles with an average size of 3.2 nm embedded in nitrogen-doped hollow porous carbon polyhedrons (abbreviated as Pt@NHPCP). The approach utilizes metal-organic frameworks (MOFs) as sacrificial template materials and a polymer as the structure stabilizer via a combined procedure involving encapsulation of Pt within MOFs, coating of a polymer shell and a thermal treatment process. Interestingly, Pt@NHPCP displays a unique hollow nanostructure with an exterior conformal shape, an interior hierarchical pore system and most importantly, high dispersion of Pt nanoparticles, and exhibits superior HER activity to the state-of-the-art commercial Pt/C catalyst. Significantly, Pt@NHPCP demonstrates excellent stability and durability, showing no nanostructure change and insignificant activity decrease in catalyzing HER after 5000 potential cycles, while severe aggregation and substantial activity loss occur in the commercial Pt/C catalyst under the same catalysis conditions.

## 2. Experimental section

### 2.1. Preparation of Pt nanoparticles

Pt nanoparticles were synthesized according to the published literature with a slight modification [33]. In a typical synthesis of Pt nanoparticles, PVP (polyvinyl pyrrolidone, 133 mg, Mw = 29,000), methanol (45 mL), and aqueous solution of $H_2PtCl_6$ (6.0 mM, 5 mL) were mixed in a flask and refluxed at 80 °C for 3 h. After that, methanol was removed by evaporation at 60 °C. The Pt nanoparticles in the remaining solution were precipitated with acetone and then collected by centrifugation. The products were cleaned with chloroform and hexane to remove excess PVP, and finally stored in 5 mL methanol for further use.

### 2.2. Preparation of Pt@ZIF-8

In a typical synthesis of Pt@ZIF-8, the above Pt nanoparticle solution (3 mL), 2-methylimidazole (4 g), and methanol (50 mL) were homogeneously mixed in a beaker. Then, a methanol solution (30 mL) containing $Zn(NO_3)_2$ $6H_2O$ (1.68 g) was added into the above solution under vigorous stirring. After 1 h, the stirring was stopped and the mixture was kept in static state for 24 h. The products were collected by centrifugation and washed with methanol several times, followed by vacuum drying overnight.

### 2.3. Preparation of Pt@NHPCP

In a typical synthesis of Pt@NHPCP, tannic acid (3 mL, 24 mM) was adjusted to pH around 8 by adding KOH aqueous solution (6 M). Then, an aqueous solution (10 mL) containing Pt@ZIF-8 (150 mg) was poured into the tannic acid solution under stirring. After 6 min, Pt@ZIF-8@TA was collected by centrifugation, washed with methanol three times, and dried in vacuum overnight. Finally, Pt@NHPCP was obtained by calcining Pt@ZIF-8@TA under an argon flow at 800 °C for 2 h. From the inductively coupled plasma-atomic emission spectrometry (ICP-AES) result, the Pt loading in synthesized Pt@NHPCP is 3.6 wt%

### 2.4. Characterization

X-ray diffraction (XRD) patterns were collected on a XRG 3000 diffractometer equipped with Cu Kα radiation. Scanning electron microscopy (SEM) experiments were carried out on LEO FESEM 1530 and S-4800 electron microscope. Transmission electron microscopy (TEM) images were collected on a JEOL 2010F microscope. The nitrogen adsorption and desorption isotherms were measured by using a Micromeritics ASAP 3020 system. Before the adsorption/desorption measurements, the samples were outgassed overnight at 180 °C. The Brunauer-Emmett-Teller (BET) specific surface area was evaluated from adsorption data in the relative pressure range of 0.1–0.3. The amount of catalysts was determined by inductively coupled plasma atomic emission spectroscopy (Perkin Elmer Ltd., USA).

### 2.5. Electrochemical measurements

A three-electrode cell was used to conduct the electrochemical measurements. A platinum wire was used as a counter electrode and a reversible hydrogen electrode was used as a reference electrode. The working electrode was a glassy-carbon Rotating Disk Electrode (RDE, diameter: 5 mm, area: 0.196 $cm^2$). The Pt loading of all samples on glassy-carbon was 2.0 μg $cm^{-2}$. Polarization curves were collected in 0.1 M $HClO_4$ solutions at a rotation rate of 1600 rpm with a sweep rate of 5 mV $s^{-1}$. The durability tests were performed at room temperature in 0.1 M $HClO_4$ solution by applying cyclic potential sweeps between 0 and −0.3 V versus a reversible hydrogen electrode (RHE) at a sweep rate of 100 mV $s^{-1}$ for 5000 cycles.

## 3. Results and discussion

Our synthetic strategy to prepare Pt@NHPCP is illustrated in Fig. 1. ZIF-8, a typical Zn-containing MOF, was selected as a sacrificial material in this work due to its high porosity and high nitrogen content as well as its facile and mild synthesis process [34,35]. Pt nanoparticles embedded in ZIF-8 (abbreviated as Pt@ZIF-8) was firstly prepared via self-assembled nucleation of ZIF-8 around as-synthesized Pt nanoparticles (Fig. 1a-c). Subsequently, Pt@ZIF-8 was coated with a thin polymer shell layer of tannic acid (abbreviated as Pt@ZIF-8@TA) by dispersing Pt@ZIF-8 into an aqueous solution of tannic acid with a pH value of about 8 (Fig. 1d). After calcination of Pt@ZIF-8@TA at 800 °C under a protective atmosphere of inert argon, Pt@NHPCP was finally obtained (Fig. 1e).

TEM imaging indicates that the as-synthesized Pt nanoparticles have an average size of 2.7 nm (Fig. S1a, b). After embedding Pt nanoparticles into ZIF-8, Pt@ZIF-8 exhibits a typical polyhedral shape with a uniform size of about 200 nm (Fig. S2), and Pt nanoparticles are highly dispersed within the pores of ZIF-8 (Fig. S3). The XRD peak intensities and positions of Pt@ZIF-8 are similar to those of pure ZIF-8 (Fig. S4a, b), which was synthesized using the same procedure in the absence of Pt nanoparticles. This indicates that the crystalline structure of ZIF-8 frameworks in Pt@ZIF-8 remains intact after embedment of Pt. No characteristic peaks for Pt are observed in the XRD pattern of Pt@ZIF-8, which can be ascribed to the relatively low Pt content and the shielding effect of the MOFs peaks in the XRD pattern. From the $N_2$ absorption-desorption data (Fig. S5a, b, and Table S1), both the BET surface area and pore volume of Pt@ZIF-8 exhibit a large decrease in comparison with pure ZIF-8, demonstrating the successful encapsulation of Pt nanoparticles within the cavities of the ZIF-8 frameworks. As shown in Fig. S6, Pt@ZIF-8@TA displays a clear core-shell nanostructure with a conformal shell layer of several nanometers, which is formed by directly replicating the polyhedral shape of the Pt@ZIF-8 core. It is found that the XRD pattern of Pt@ZIF-8@TA remains unchanged after coating of tannic acid (Fig. S4c), indicating the preservation of the original ZIF-8 framework.

As shown in Fig. 2a, b, Pt@NHPCP exhibits a polyhedral

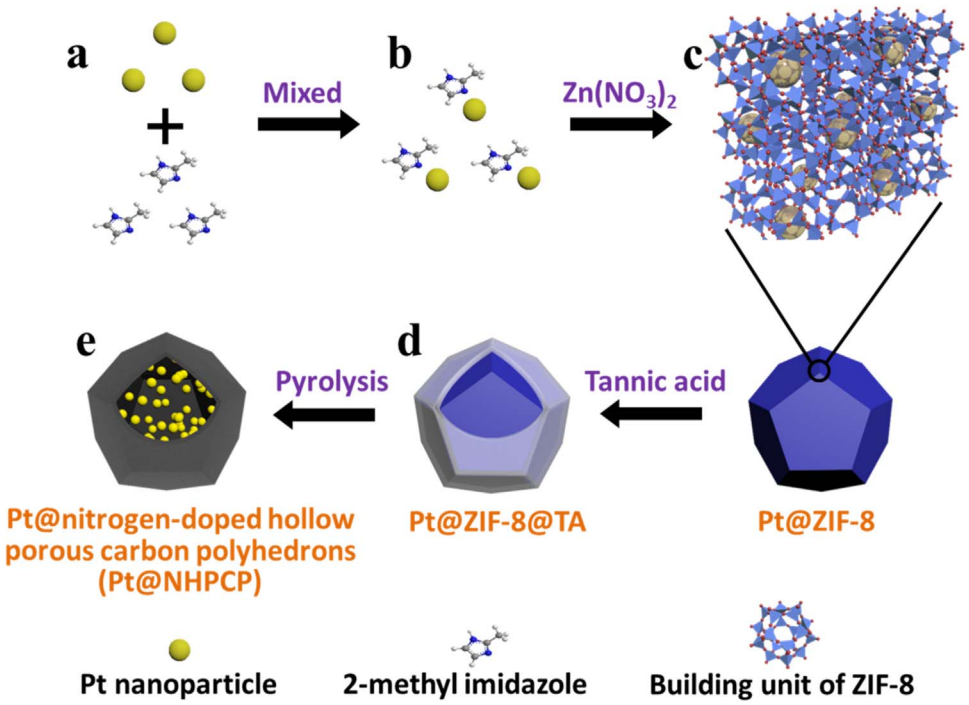


**Fig. 1.** Schematic illustration of the fabrication of Pt@NHPCP.

morphology with an average size of about 220 nm, indicating the retention of the conformal shape after thermal treatment of Pt@ZIF-8@TA. Interestingly, the TEM image of Pt@NHPCP exhibits a unique hollow structure with a thin conformal shell and a porous nanostructured core (Fig. 2c). In addition, pyrolysis of Pt@ZIF-8 under the same conditions results in generating dense particles (Fig. S7), indicating that the TA is crucial for the formation of hollow porous nanostructures. The high-resolution TEM (HRTEM) image of Pt@NHPCP shows that fine nanoparticles are homogeneously dispersed within the entire porous nanostructure (Fig. 2d). The highly porous nature and high dispersion of nanoparticles in Pt@NHPCP are clearly presented in the high-angle annular dark-field scanning TEM (HAADF-STEM) images (Fig. 2e, f). Compared to the pristine nanoparticles, the average size of these nanoparticles increases slightly from 2.7 to 3.2 nm (Fig. S8), which could be caused by the high temperature treatment. A HRTEM image of an individual nanoparticle clearly reveals lattice fringes with an interplanar spacing of 0.22 nm (Fig. S9), corresponding to the (111) planes of face-centered cubic (fcc) Pt. The energy dispersive X-ray spectroscopy (EDX) elemental mapping images of Pt@NHPCP in Fig. 2g-j not only display the homogeneous dispersion of Pt throughout the whole composite material, but also disclose the nature of nitrogen-doping for this hollow porous carbon support. To further investigate the nitrogen-doping in Pt@NHPCP, X-ray photoelectron spectroscopy (XPS) was employed. The N 1 s spectra for Pt@NHPCP can be deconvoluted into four obvious peaks (Fig. S10), corresponding to pyridinic (398.6 eV), pyrrolic (400.1 eV), graphitic (401.2 eV), and oxidized (403.2 eV) nitrogen species, respectively. The XPS elemental analysis result reveals that Pt@NHPCP contains a high nitrogen content of 12.4 at% with pyridinic N as the dominant nitrogen species. Notably, both high nitrogen content in carbon materials and the formation of pyridinic N have been demonstrated to provide beneficial catalyst-support interactions between Pt nanoparticles and carbon supports, which could substantially improve catalyst activity and stability [36,37]. Moreover, compared to the Pt@ZIF-8, the binding energy of Pt 4 f from Pt@NHPCP shows an obvious shift to higher energy (Fig. S11), which is caused by the interactions between Pt and support due to the presence of N sites [37]. In the XRD pattern of Pt@NHPCP (Fig. S4d), the diffraction peaks between 30° and 90° are well-indexed to the typical (111), (200), (220) and (311) reflections of Pt crystals with fcc structure (PDF No. 04–0802), while the broadened diffraction peak at 2 theta at around 25° can be assigned to the carbon supports. It is noteworthy that the diffraction peaks for Pt are broad, indicating the small particle size of Pt, which is in good agreement with the TEM result. In addition, there is no diffraction peak for Zn because of the evaporation of Zn metal during the pyrolysis process [38]. Furthermore, the porous nanostructure of Pt@NHPCP was further studied by $N_2$ adsorption/desorption measurement (Fig. S5c), revealing a large BET surface area of 516 $m^2 g^{-1}$. Notably, the pore size distribution of Pt@NHPCP reflects four distinct pore sizes centered at 3.4, 13.6, 34.5, and 70.4 nm (Fig. S12), indicating the hierarchical pore system of hollow porous carbon polyhedrons, which can benefit catalytic processes by facilitating mass transport.

The above structural analyses fully confirm the formation of highly dispersed Pt nanoparticles embedded in nitrogen-doped hollow porous polyhedrons derived from polymer covered metal-organic frameworks via thermal treatment process. In comparison with the previously reported metal nanoparticles in the interior of hollow porous carbons, the resulting Pt@NHPCP has several advantages: i) simple and efficient synthesis technique, which does not require harsh synthesis conditions, such as strongly corrosive acids or bases, and is thereby highly desirable for commercial applications; ii) high dispersion of metal nanoparticles, which can maximize the utilization of the metal catalyst; iii) large surface area from hollow carbons with interior hierarchical porous nanostructure, which can greatly facilitate the mass transport in catalytic processes; iv) high content of nitrogen dopant, which can further enhance catalyst activity and stability.

The HER performance of Pt@NHPCP was investigated by using linear sweep voltammetry at a scan rate of 5 mV $s^{-1}$ in 0.1 M $HClO_4$ at room temperature. For comparison, commercial Pt/C catalyst was also tested under the same conditions as the reference. Fig. 3a shows the HER polarization curves of Pt@NHPCP and commercial Pt/C. Pt@NHPCP displays an onset potential of −2.7 mV, which is much more positive than that of commercial Pt/C (−7.5 mV; Fig. 3b). Meanwhile, it is clearly revealed that the current density of Pt@NHPCP is larger than that of commercial Pt/C at the same operating potential. For instance, at a current density of 10 mA $cm^{-2}$, the operating potential is measured to be −57.0 mV for Pt@NHPCP, while commercial Pt/C shows a more negative operating potential of −69.6 mV (Fig. 3b). To gain insights into the mechanism of the catalytic

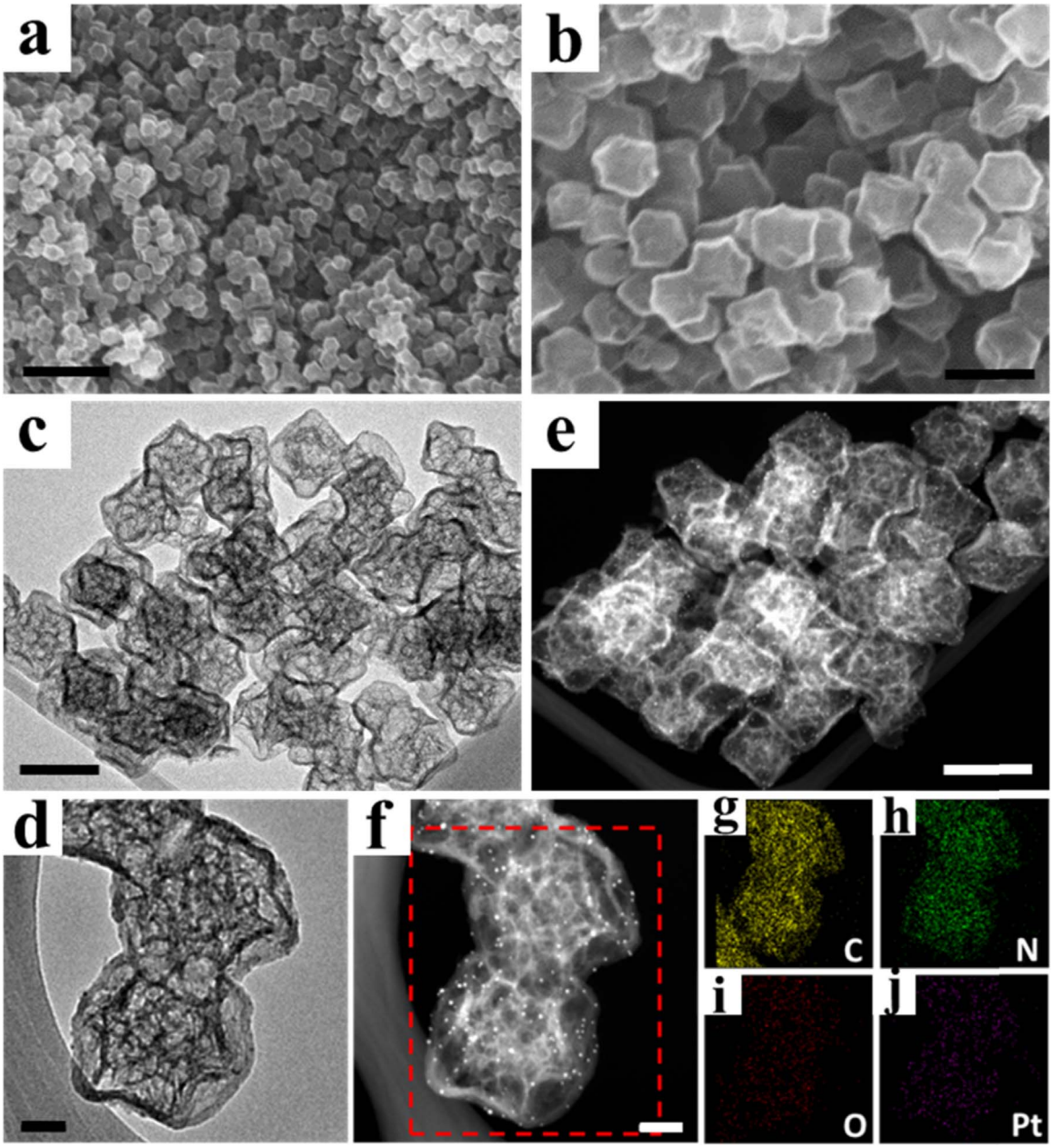


**Fig. 2.** (a) Low-resolution SEM, (b) high-resolution SEM, (c) low-resolution TEM, (d) high-resolution TEM, (e) low-resolution HAADF-STEM, and (f) high-resolution HAADF-STEM images of Pt@NHPCP. (g-j) Elemental mapping results of the zone indicated in (f): (g) C (yellow), (h) N (green), (i) O (red), and (j) Pt (purple). Scale bars are (a) 1 μm, (b) 300 nm, (c,e) 200 nm and (d, f) 50 nm.

activity of Pt@NHPCP and commercial Pt/C for HER, reaction kinetics was evaluated from the Tafel plots. The Tafel slope of Pt@NHPCP was calculated to be 27 mV $dec^{-1}$, which is much lower than that of commercial Pt/C (32 mV $dec^{-1}$; Fig. 3c). The low Tafel slope of Pt@NHPCP reveals that the rate-limiting step in HER is the Tafel recombination process, i.e., the Volmer-Tafel mechanism [2,39]. In addition, the current density of pure NHPCP is negligible in comparison with Pt@NHPCP (Fig. 3d), indicating that the catalytic activity of Pt@NHPCP is mainly attributable to the embedded Pt nanoparticles. These results demonstrate that Pt@NHPCP displays a superior HER activity compared to commercial Pt/C.

Moreover, the electrochemical stability of Pt@NHPCP and commercial Pt/C was also evaluated by performing linear potential sweeps between 0 and −0.3 V versus RHE at room temperature in 0.1 M $HClO_4$ with a sweep rate of 100 mV $s^{-1}$. After 5000 cycles, a very slight potential shift of the polarization curve is observed for Pt@NHPCP (Fig. 4a), while commercial Pt/C shows a large potential shift to lower current density (Fig. 4b), indicating the catalytic stability of Pt@NHPCP is also much better than that of commercial Pt/C. As shown in Fig. 4c, only 0.9 mV potential shift in onset potential for Pt@NHPCP is displayed after 5000 cycles compared with 13.3 mV onset potential shift for commercial Pt/C. Moreover, the overpotential of Pt@NHPCP displays a slight potential shift of 5.2 mV at the current density of 10 mA $cm^{-2}$ after 5000 cycles. By comparison, the overpotential shift for commercial Pt/C is 27.7 mV. Thus, with regard to the onset potential and overpotential, Pt@NHPCP exhibits much better stability than commercial Pt/C. Notably, after 5000 cycles, the Tafel slope of Pt@NHPCP (33 mV $dec^{-1}$) is still much lower than that of commercial Pt/C (40 mV $dec^{-1}$; Fig. 4d), indicating the much higher HER activity of Pt@NHPCP than commercial Pt/C even after durability tests. These results definitively confirm that Pt@NHPCP has an excellent HER durability in comparison with commercial Pt/C.

To further illuminate the reason for the different degradation levels

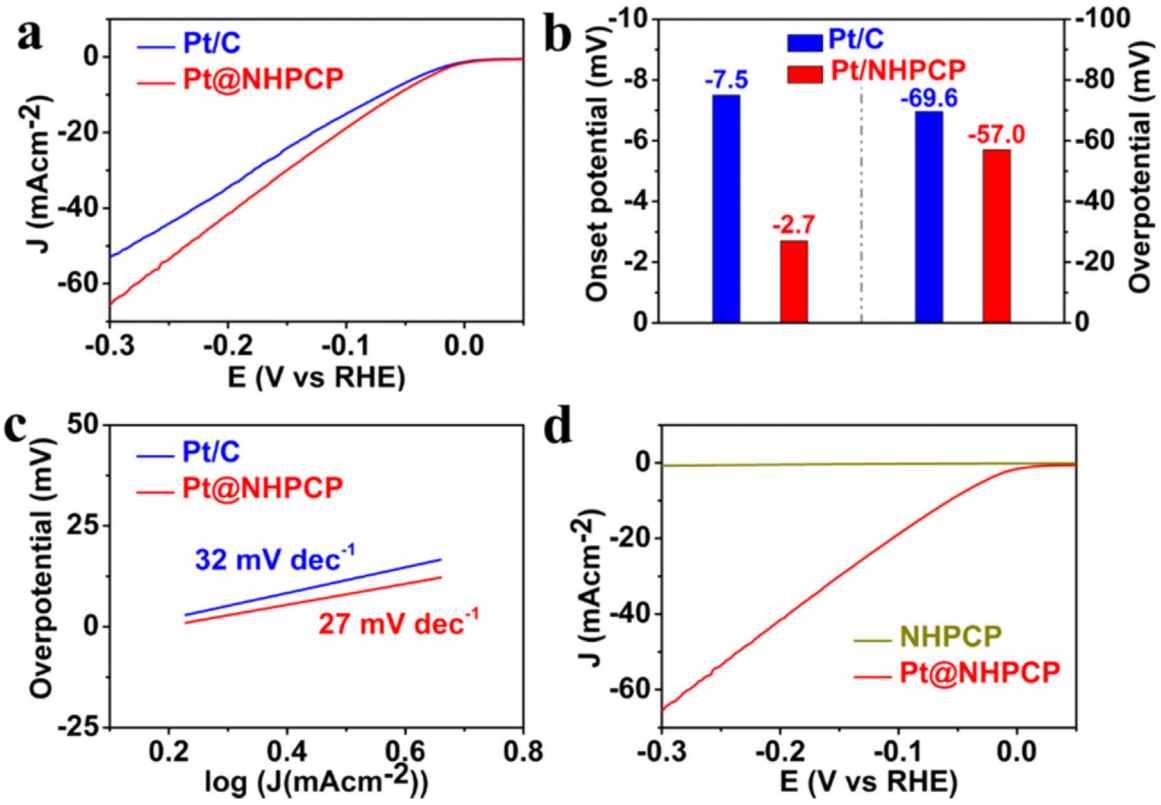


**Fig. 3.** (a) Polarization curves of Pt@NHPCP and commercial Pt/C for HER in 0.1 M $HClO_4$ with a potential scan rate of 5 mV $s^{-1}$. (b) Onset potentials and overpotentials (at current density of 10.0 mA $cm^{-2}$) of Pt@NHPCP and commercial Pt/C. (c) Corresponding Tafel plots for the data presented in (a). (d) Polarization curves of Pt@NHPCP and pure NHPCP.

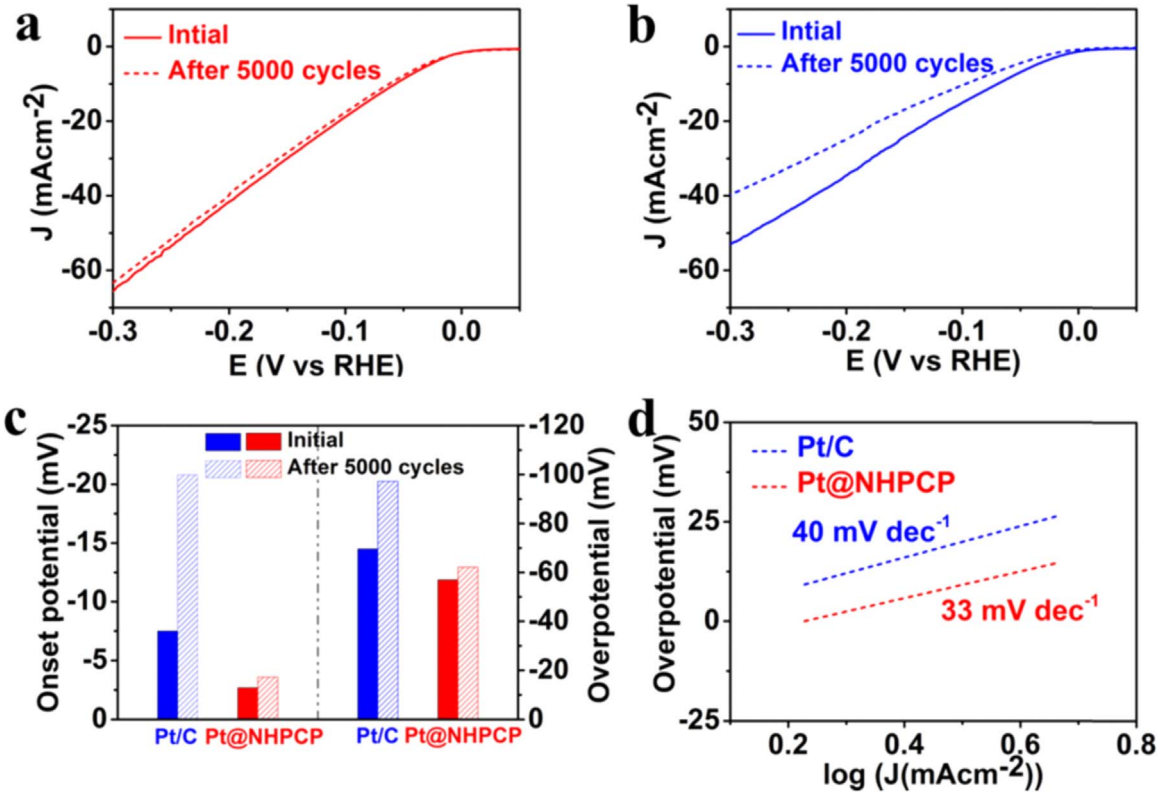


**Fig. 4.** Polarization curves of (a) commercial Pt/C and (b) Pt@NHPCP before and after 5000 potential cycles in 0.1 M $HClO_4$ solution with a sweep rate of 100 mV $s^{-1}$. (c) Onset potentials and overpotentials (at current density of 10.0 mA $cm^{-2}$) of Pt@NHPCP and commercial Pt/C before and after 5000 potential cycles. (d) Tafel plots of Pt@NHPCP and commercial Pt/C after 5000 potential cycles.

of Pt@NHPCP and commercial Pt/C, their morphological and structural changes after durability tests were investigated. Impressively, there is no obvious change of shape, morphology, porous nanostructure, and Pt metal size and distribution for Pt@NHPCP after 5000 cycles (see Fig. S13a, b), while commercial Pt/C shows serious ripening and aggregation (Fig. S13c, d). This indicates that Pt nanoparticles dispersed within nitrogen-doped hollow porous carbons are incredibly stable toward electrocatalytic HER. Together, our studies clearly demonstrate the excellent activity, stability and durability of the obtained Pt@NHPCP, which can be reasonably ascribed to synergistic effects of the catalyst and support material. On the one hand, with high dispersion and small size, the former can maximize the utilization of Pt as well as enhance the intrinsic activity and stability. On the other hand, the later possesses the features of nitrogen-doping, large surface area, hollow structure, and hierarchical pore system, all of which can stabilize the Pt catalyst and facilitate mass transport and diffusion, thereby improving its activity and durability.

## 4. Conclusions

In summary, we have developed a novel and efficient strategy to prepare highly dispersed Pt nanoparticles embedded within unique nitrogen-doped hollow porous carbon polyhedrons derived from polymer coated metal-organic frameworks. Compared to commercial Pt/C catalyst, the as-synthesized Pt@NHPCP exhibits enhanced activity and excellent stability and durability for catalyzing HER. Significantly, Pt@NHPCP shows no obvious changes in shape, porous nanostructure, Pt metal size and distribution as well as negligible decrease in activity after 5000 cycles. The outstanding performance toward HER could be attributed to the high dispersion of Pt, nitrogen dopant, large surface area, hollow structure and hierarchical pore feature exhibited by the unique nanostructures. The synthesis strategy described herein is simple and scalable and it opens a new avenue to fabricate catalytically-active nanoparticles within heteroatom-doped hollow porous nanostructures, which could be highly desirable catalysts for many chemical and electrochemical reactions.

## Acknowledgments

This work was supported by the Natural Sciences and Engineering Research Council of Canada (NSERC), the University of Waterloo, and the Waterloo Institute for Nanotechnology. The authors greatly acknowledge the Catalysis Research for Polymer Electrolyte Fuel Cells (CaRPE FC) Network administered from Simon Fraser Grant No. APCPJ 417858-11 through NSERC. TEM imaging was performed at the Canadian Center for Electron Microscopy (CCEM) located at McMaster University.

## Appendix A. Supporting information

Supplementary data associated with this article can be found in the online version at http://dx.doi.org/10.1016/j.nanoen.2017.07.032.

## References

[1] M.G. Walter, E.L. Warren, J.R. McKone, S.W. Boettcher, Q. Mi, E.A. Santori, N.S. Lewis, Chem. Rev. 110 (2010) 6446–6473.
[2] W.-F. Chen, J.T. Muckerman, E. Fujita, Chem. Commun. 49 (2013) 8896–8909.
[3] N.S. Lewis, D.G. Nocera, P. Natl. Acad. Sci. USA 103 (2006) 15729–15735.
[4] D.G. Nocera, Acc. Chem. Res. 45 (2012) 767–776.
[5] Q. Lu, Y. Yu, Q. Ma, B. Chen, H. Zhang, Adv. Mater. 28 (2016) 1917–1933.
[6] J.A. Turner, Science 305 (2004) 972–974.
[7] P. Wang, X. Zhang, J. Zhang, S. Wan, S. Guo, G. Lu, J. Yao, X. Huang, Nat. Commun. 8 (2017) 14580.
[8] Y. Ito, W. Cong, T. Fujita, Z. Tang, M. Chen, Angew. Chem. Int. Ed. 54 (2015) 2131–2136.
[9] M. Li, Q. Ma, W. Zi, X. Liu, X. Zhu, S.F. Liu, Sci. Adv. 1 (2015) e1400268.
[10] S. Wang, X. Gao, X. Hang, X. Zhu, H. Han, W. Liao, W. Chen, J. Am. Chem. Soc. 138 (2016) 16236–16239.
[11] X. Zou, X. Huang, A. Goswami, R. Silva, B.R. Sathe, E. Mikmeková, T. Asefa, Angew. Chem. 126 (2014) 4461–4465 (Angew. Chem. Int. Ed. 53, )2014, pp. 4372–4376).
[12] P. Xiao, M.A. Sk, L. Thia, X. Ge, R.J. Lim, J.-Y. Wang, K.H. Lim, X. Wang, Energy Environ. Sci. 7 (2014) 2624–2629.
[13] B. Cao, G.M. Veith, J.C. Neuefeind, R.R. Adzic, P.G. Khalifah, J. Am. Chem. Soc. 135 (2013) 19186–19192.
[14] E.J. Popczun, C.G. Read, C.W. Roske, N.S. Lewis, R.E. Schaak, Angew. Chem. Int. Ed. 53 (2014) 5427–5430.
[15] Z. Fan, Z. Luo, X. Huang, B. Li, Y. Chen, J. Wang, Y. Hu, H. Zhang, J. Am. Chem. Soc. 138 (2016) 1414–1419.
[16] D. Higgins, M.A. Hoque, M.H. Seo, R. Wang, F. Hassan, J.Y. Choi, M. Pritzker, A. Yu, J. Zhang, Z. Chen, Adv. Funct. Mater. 24 (2014) 4325–4336.
[17] J. Ying, X.-Y. Yang, Z.-Y. Hu, S.-C. Mu, C. Janiak, W. Geng, M. Pan, X. Ke, G. Van Tendeloo, B.-L. Su, Nano Energy 8 (2014) 214–222.
[18] J. Ying, Z.-Y. Hu, X.-Y. Yang, H. Wei, Y.-X. Xiao, C. Janiak, S.-C. Mu, G. Tian, M. Pan, G. Van Tendeloo, Chem. Commun. 52 (2016) 8219–8222.
[19] S. Ikeda, S. Ishino, T. Harada, N. Okamoto, T. Sakata, H. Mori, S. Kuwabata, T. Torimoto, M. Matsumura, Angew. Chem. Int. Ed. 45 (2006) 7063–7066.
[20] R. Liu, S.M. Mahurin, C. Li, R.R. Unocic, J.C. Idrobo, H. Gao, S.J. Pennycook, S. Dai, Angew. Chem. Int. Ed. 50 (2011) 6799–6802.
[21] C. Galeano, C. Baldizzone, H. Bongard, B. Spliethoff, C. Weidenthaler, J.C. Meier, K.J. Mayrhofer, F. Schüth, Adv. Funct. Mater. 24 (2014) 220–232.
[22] C. Galeano, J.C. Meier, M. Soorholtz, H. Bongard, C. Baldizzone, K.J. Mayrhofer, F. Schüth, ACS Catal. 4 (2014) 3856–3868.
[23] G.-H. Wang, J. Hilgert, F.H. Richter, F. Wang, H.-J. Bongard, B. Spliethoff, C. Weidenthaler, F. Schüth, Nat. Mater. 13 (2014) 293–300.
[24] Y. Zhou, K. Neyerlin, T.S. Olson, S. Pylypenko, J. Bult, H.N. Dinh, T. Gennett, Z. Shao, R. O'Hayre, Energ. Environ. Sci. 3 (2010) 1437–1446.
[25] M.A. Hoque, F.M. Hassan, D. Higgins, J.Y. Choi, M. Pritzker, S. Knights, S. Ye, Z. Chen, Adv. Mater. 27 (2015) 1229–1234.
[26] R. Wang, D.C. Higgins, M.A. Hoque, D. Lee, F. Hassan, Z. Chen, Sci. Rep. 3 (2013) 2431.
[27] M.A. Hoque, F.M. Hassan, M.-H. Seo, J.-Y. Choi, M. Pritzker, S. Knights, S. Ye, Z. Chen, Nano Energy 19 (2016) 27–38.
[28] S. Chen, J. Bi, Y. Zhao, L. Yang, C. Zhang, Y. Ma, Q. Wu, X. Wang, Z. Hu, Adv. Mater. 24 (2012) 5593–5597.
[29] J. Han, G. Xu, B. Ding, J. Pan, H. Dou, D.R. MacFarlane, J. Mater. Chem. A2 (2014) 5352–5357.
[30] W. Zhou, X. Xiao, M. Cai, L. Yang, Nano Lett. 14 (2014) 5250–5256.
[31] G. Zhou, Y. Zhao, A. Manthiram, Adv. Energy Mater. 5 (2015) 1402263.
[32] S. Feng, W. Li, Q. Shi, Y. Li, J. Chen, Y. Ling, A.M. Asiri, D. Zhao, Chem. Commun. 50 (2014) 329–331.
[33] T. Teranishi, M. Hosoe, T. Tanaka, M. Miyake, J. Phys. Chem. B 103 (1999) 3818–3827.
[34] J. Tang, R.R. Salunkhe, J. Liu, N.L. Torad, M. Imura, S. Furukawa, Y. Yamauchi, J. Am. Chem. Soc. 137 (2015) 1572–1580.
[35] G. Lu, S. Li, Z. Guo, O.K. Farha, B.G. Hauser, X. Qi, Y. Wang, X. Wang, S. Han, X. Liu, Nat. Chem. 4 (2012) 310–316.
[36] G. Wu, D. Li, C. Dai, D. Wang, N. Li, Langmuir 24 (2008) 3566–3575.
[37] D. He, Y. Jiang, H. Lv, M. Pan, S. Mu, Appl. Catal., B 132 (2013) 379–388.
[38] A.J. Amali, J.-K. Sun, Q. Xu, Chem. Commun. 50 (2014) 1519–1522.
[39] Z.W. Seh, J. Kibsgaard, C.F. Dickens, I. Chorkendorff, J.K. Nørskov, T.F. Jaramillo, Science 355 (2017) (eaad4998).

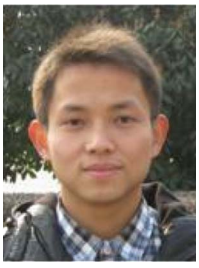

**Dr. Jie Ying** received his Ph.D. degree from Wuhan University of Technology under the supervision of Prof. Bao-Lian Su and Prof. Xiao-Yu Yang in 2016. Currently, he has been a postdoctoral research fellow with Prof. Zhongwei Chen in the Department of Chemical Engineering at University of Waterloo, Canada. His current work includes design and synthesis of nanocomposites, catalysis, and electrocatalysis.

**Gaopeng Jiang** received his master's degree from Donghua University in 2012 and currently is the Ph.D. candidate on Chemical Engineering (Nanotechnology) in University of Waterloo, Canada. His research interest mainly focuses on the design and development of nanostructured materials for energy storage and conversion devices including fuel cells, batteries and sensors.

**Zachary Paul Cano** received his Bachelor's degree (2012) and Master's degree (2015) in Materials Science and Engineering from McMaster University, where he specialized in corrosion science. He is now pursuing his Ph.D. in Chemical Engineering (Nanotechnology) under the supervision of Prof. Michael Fowler and Prof. Zhongwei Chen at the University of Waterloo. His research is currently focused on the development of novel electrode structures and cell designs for long-lasting rechargeable metal-air batteries.

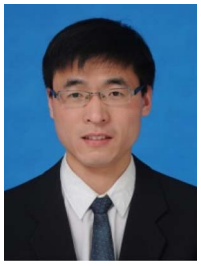

**Dr. Lei Han** received his bachelor degree from the Department of Chemistry, Zhengzhou University, P. R. China (2009). In 2009, he then joined Professor Shaojun Dong's group at the Changchun Institute of Applied Chemistry, Chinese Academy of Sciences, and received his Ph.D. degree in 2015. Currently, he has been a postdoctoral research fellow with Professor Zhongwei Chen in the Department of Chemical Engineering at University of Waterloo (Canada). His main research interests are focused on photoelectrochemistry and oxygen electrochemistry.

**Dr. Xiao-Yu Yang** received his Ph.D. from Jilin University (co-educated at the University of Namur, Belgium). In 2007, he held a post-doctoral position at the University of Namur with Prof. Bao-Lian Su working on hierachically porous materials. He is currently a "Chargé de Recherches" of the F.N.R.S. (National Foundation of Scientific Research). He got an honour of "Chutian scholar" at Wuhan University of Technology in 2010. His research is aimed at new synthesis pathways towards novel porous systems, catalysts, bio-nanoreactors, bio-inspired materials and biofuel cells.

**Dr. Zhongwei Chen** is Canada Research Chair Professor in Advanced Materials for Clean Energy at University of Waterloo. His research interests are in the development of advanced energy materials for metal-air batteries, lithium-ion batteries and fuel cells. He has published 1 book, 7 book chapters and more than 150 peer reviewed journal articles with over 10,000 citations with H-index 50 (GoogleScholar). He is also listed as inventor on 15 US/international patents, with several licensed to companies in USA and Canada. He was recipient of the 2016 E. W. R Steacie Memorial Fellowship, which followed shortly upon several other prestigious honors, including the Ontario Early Researcher Award, an NSERC Discovery Supplement Award, the Distinguished Performance and the Research Excellence Awards from the University of Waterloo.